Alternate Analysis of an In Vitro Solubility Study on the Lung Dissolution Rate of 238PuO2 Material Involved in the 2020 Incident at Los Alamos National Laboratory

Miller, Guthrie
de Souza Zanotta Dumit, Sara
Poudel, Deepesh
Klumpp, John Allan

To be published in: Health Physics

DOI to publisher's version: 10.1097/HP.0000000000001621

ALTERNATE ANALYSIS OF AN IN VITRO SOLUBILITY STUDY ON THE LUNG DISSOLUTION RATE OF $^{238}PuO_2$ MATERIAL INVOLVED IN THE 2020 INCIDENT AT LOS ALAMOS NATIONAL LABORATORY

Guthrie Miller[1], Sara Dumit[2], Deepesh Poudel[2], John Klumpp[2]
[1]*Unaffiliated (retired from Los Alamos National Laboratory), Santa Fe, NM, USA*
[2]*Los Alamos National Laboratory, Radiation Protection Division, Los Alamos, NM 87545, USA*

Corresponding Author:
Dr. Sara Dumit
Los Alamos National Laboratory
Radiation Protection Division
Internal Dosimetry, MS G761
Los Alamos, NM 87545
United States of America
Email: sarad@lanl.gov

ABSTRACT

This work presents an alternate analysis of an in vitro solubility study on the lung dissolution rate of $^{238}PuO_2$ material involved in a recent inhalation incident at Los Alamos National Laboratory (LANL). The original dataset used in this work was retrieved from a recently published report by LaMont et al. (2022). The present work shows an analysis of the same dataset by modeling the dissolution in separate time-intervals rather than modeling the cumulative dissolution.

Keywords: analysis, statistical; inhalation; model; ^{238}Pu.

INTRODUCTION

In June of 2020, an accidental inhalation of plutonium occurred at Los Alamos National Laboratory (LANL) (LaMont et al. 2022). The details of the incident have already been described in-depth elsewhere (Dumit et al. 2022; LaMont et al. 2022; Poudel et al. 2022). Following the incident, an investigation about the solubility of the material took place at LANL's radiochemistry laboratory, C-NR, which analyzed the plutonium material collected from a fixed air monitor located above the workstation of the radiation workers (LaMont et al. 2022). The study found that the material was 99% insoluble and 1% soluble, *"approximately 1% of material [dissolved] quickly, and 99% of the material [dissolved] very slowly, with a half-time of approximately 120 years."* This work presents an alternate analysis of the same dataset by modeling the dissolution in separate time-intervals rather than modeling the cumulative dissolution.

ALTERNATE ANALYSIS OF SOLUBILITY STUDY DATA

For the solubility study, an air filter from a fixed head air sampler (FAS) mounted over the place of the release was cut into four quarters. LaMont et al. 2022 described that each of the four quarters were placed into separate containers of simulated lung fluid (SLF). The SLF used in their study was prepared according to the Moss formula and the containers used were designed to allow free and full contact of the samples with the SLF. Moreover, the containers' configuration also allowed easy separation of the SLF fractions collected during the experiment. The full description of the experiment can be found in

the report published by LaMont et al. 2022. But briefly, the samples were continuously agitated inside an incubator, at 37 °C temperature, and 5% CO_2 atmosphere (with pH stabilized at 7.2 – 7.4). The experiment duration comprised 134 days, consisting of SLF fraction collections at particular time points (0.015, 0.055, 0.23, 1.07, 5.1, 20.1, 43, 77, 102 [77 days + 600 hours], and 134 days), and also of samples being transferred to fresh SLF at the same time points. It must be noted that the SLF used was prepared either on the day of, or one day prior to the sample handling (LaMont et al. 2022).

The experimental data consisted of measurements of the fractions of the initial activity going into solution of SLF from the 4 filter quarters in the time intervals shown in Table 1. The 134 day was not used in this analysis to correspond to what was done in the original analysis by LaMont et al. 2022. The measurements of the 4 quarters were combined to produce a single logarithmic average and standard deviation. Time t refers to the end time of the interval.

Table 1. Dissolution data used. The quantities t_0 and t are the beginning and end times of the interval, dissolved fraction is the logarithmic average (exp(<ln..>)) over the 4 samples of the fraction of material dissolved in that time interval, cumulative is the cumulative amount dissolved, and S is the logarithmic standard deviation of the dissolved fractions for the 4 samples.

Time (days)		**Interval**	**Dissolved fraction ($\times 10^{-5}$)**	**S**	**Cumulative**
t_0	**t**				
0	0.015	22 m	671	0.128	0.0067
0.015	0.055	58 m	146	0.093	0.0082
0.055	0.23	252 m	81	0.623	0.0090
0.23	1.07	20 h	18.6	0.282	0.0092
1.07	5.1	97 h	3.4	0.398	0.0092
5.1	20.1	360 h	26.4	0.451	0.0095
20.1	43	550 h	4.1	0.616	0.0095
43	77	816 h	3.6	1.431	0.0095
77	102	600 h	3.7	1.089	0.0096

For ease of visualization the data may be used to produce an approximate rate of dissolution (fraction/day) at the midpoint of the interval. These data are shown in Figure 1. The model curve is the 4-component fit discussed subsequently.

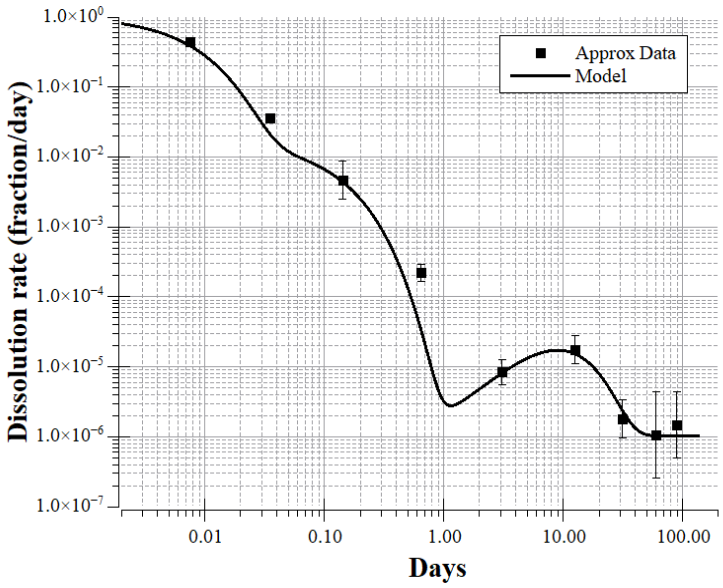

Fig. 1. Rate of dissolution, approximate data and model.

The data used in this analysis were the amounts dissolved in the exact time intervals, in the same way that "Urine 24h" used in internal dosimetry is the excretion in a certain 24-h interval. These data versus fit are shown in Figure 2. Only seven data points are shown for visual clarity.

Note that the data for dissolution in different time intervals are independent, unlike the data for the cumulative dissolution. This allows the independent data assumption that the log of the combined likelihood is the sum of χ_i^2 over the data points i=1, nData (number of data points), where χ_i^2 is defined as -2 ln(likelihood) for the i^{th} data point (Miller 2017). If the cumulative data were to be used, correlation terms would need to be included.

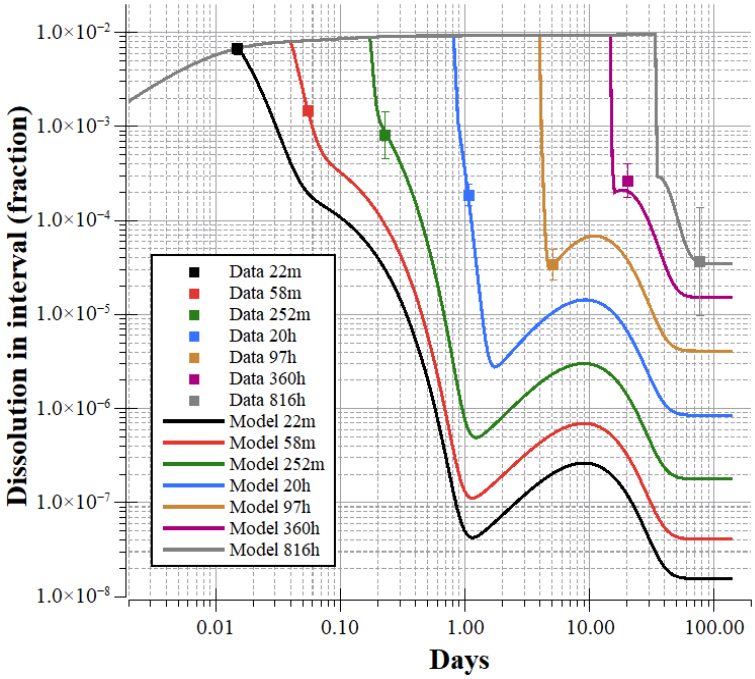

Fig. 2. Dissolution fraction data used in this analysis.

When the time is less or equal to the interval (as for the first data point), the model curve is the cumulative fraction. In the figure one can see the cumulative fraction approaching 1% at long times in agreement with the data shown in Table 1.

The empirical likelihood function based on the 4 replicate measurements given in Table 1 was used (Miller 2017); this likelihood function option (Student's t-distribution) is built into the software package used, IDode (Miller et al. 2012, 2019). In Figure 2 the data and uncertainties from Table 1 are shown. As can be seen from the fact that the fit curve departs very little from the data points in terms of the standard deviation of the data point (showing χ = +-1), the value of χ^2/nData is very small (actual value 0.16). The number of data points, nData=9.

Table 2 shows the LaMont et al. (2022) 2-component dissolution model along with the 4-component model presented here as a more accurate representation of the dataset. "Up-down" solubility behavior has been seen before with ^{238}Pu and is attributed to particle fragmentation and increased solubility caused by the high specific activity of ^{238}Pu (Diel and Mewhinney 1980; Fleischer and Raabe 1978; Hickman et al 1995; Poudel et al. 2019).

Table 2. Dissolution models considered.

Fraction (%)	Compartmental Model[a]	Rate (day^{-1})
LaMont et al. (2022) study		
99	S→out	2×10^{-6}
0.9	R→out	90
This work		
99	S→out	1.7×10^{-6}
0.71	R1→out	468
0.18	R2→out	10.4
0.0003	X→X1→X2→out	0.305[*]

[a]R Rapid, S Slow, Up-down X2 ~$(st)^2 \exp(-st)$, S=0.305/day
[*]All the rates are S=0.305

Table 3 shows the values of chain-average χ^2/nData, the Evidence Integral, which is the integral of the likelihood function over the prior, and the posterior average likelihood function.

Table 3. Analysis results.

Model	Number of parameters	χ^2/nData[a]	Evidence[b]	L[c]
2-Comp	3	7.9	3.6×10^{-19}	1.1×10^{-16}
3-Comp	5	2	2.1×10^{-9}	3.9×10^{-4}
4-Comp	7	1.2	2.5×10^{-9}	1.8×10^{-2}

[a]Chain-average χ^2/nData
[b]Integral of likelihood function over prior
[c]Chain-average likelihood

The Evidence Integral (e.g. Miller 2017) is proportional to the posterior probability of the model given the data. Likewise, with much data, it can be argued that the posterior-average likelihood estimates the posterior probability of the model given the data. The 4-component model is the only one consistent with the dataset and the uncertainties in the sense of having χ^2/nData about 1 (on-average the deviation of model calculation from data is 1 data standard deviation), and furthermore this model has the largest Evidence and average likelihood.

The prior is log-scale uniform with large extent, so the posterior is hardly influenced by the extent of the prior. The Evidence Integral is influenced by the extent of the prior and having a larger extent reduces the Evidence. A plot showing the extent of the prior relative to the posterior for the two additional variables entering in for the 4-component model is shown in Figure 3. A tighter prior box would increase the Evidence integral.

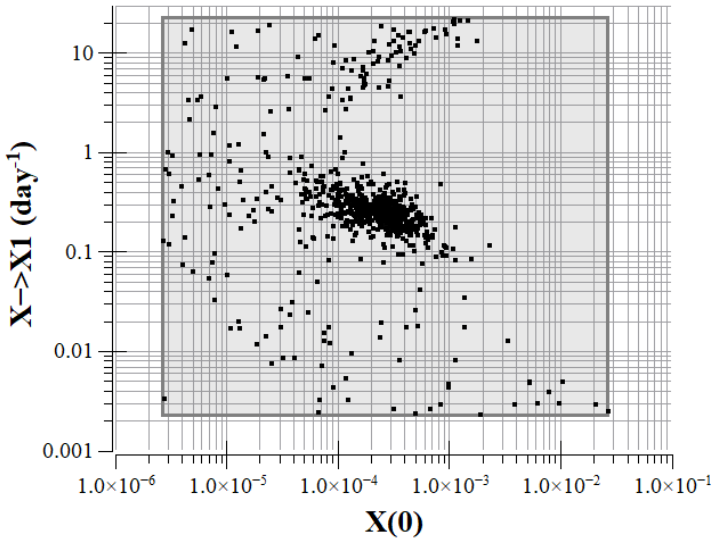

Fig. 3. Posterior probability scatter plot for additional parameters distinguishing 4-component model from 3-component model. The points represent equally likely interpretations of the data and the box shows the extent of the prior.

As seen in Figure 3, the posterior is mostly well constrained by the data but there is also another diffuse, poorly constrained component.

CONCLUSIONS

This analysis of the solubility study dataset obtained by the Los Alamos radiochemistry laboratory confirms the conclusion that the material was 99% insoluble and 1% soluble, however it also concludes that the soluble component consists of three different behaviors: two simple, rapidly-dissolving components, and a component with an up-down solubility behavior modeled by three compartments in series with equal, somewhat rapid, transport between them. The up-down type of solubility behavior has been observed before with ^{238}Pu and is attributed to increased solubility caused by increased surface area of particles as they mechanically break up because of the high specific activity of ^{238}Pu.

ACKNOWLEDGEMENTS

The authors would like to thank LANL's radiochemistry (C-NR) Team (LaMont SP, Steiner RE, Macsik Z, Hudston LA, Harris MN, Tenner TJ, Naes BE, Wurth KN) and also Dr. Luiz Bertelli for the important discussions and fruitful exchange of scientific knowledge.

REFERENCES

Diel JH, Mewhinney JA. Breakup of inhaled 238PuO2 particles in the lungs of hamsters and dogs. Inhalation Toxicology Research Institute Annual Report 1979-90, LMF-84; Albuquerque, NM 17-19; 1980.

Dumit S, Miller G, Poudel D, Bertelli L, Klumpp JA. Chelation model validation: modeling of a plutonium-238 inhalation incident treated with DTPA at Los Alamos National Laboratory. Health Phys [ideally in the same issue as the present manuscript]; 2022.

Fleischer RL and Raabe OG. Fragmentation of respirable PuO2 particles in water by alpha-decay: a mode of 'dissolution'. Solid State Nuclear Track Detectors ed F Grancer, H Patezke and E Schopper. Oxford, UK: 663-668; 1978.

Hickman AW, Griffith WC, Roessler GS, Guilmette RA. Application of a canine 238Pu biokinetics/dosimetry model to human bioassay data. Health Phys. 68: 359–70; 1995.

LaMont SP, Steiner RE, Macsik Z, Hudston LA, Harris MN, Tenner TJ, Naes BE, Wurth KN. $^{238}PuO_2$ In Vitro Lung Dissolution Rate and Particle Size Determination for Material Involved in the June 8, 2020 Incident at the Los Alamos National Laboratory PF-4 Facility. Final Report, LA-UR-22-20261. https://doi.org/10.2172/1840854. https://www.osti.gov/servlets/purl/1840854; 2022.

Miller G, Bertelli L, Klare K, Weber W, Doyle-Eisele M, Guilmette R. Software for empirical building of biokinetic models for normal and decorporation-affected data. Health Phys 103:484–494; 2012.

Miller G. Probabilistic interpretation of data—a physicist's approach. Morrisville, NC: Lulu Glasstree Publications; 2017.

Miller G, Klumpp JA, Poudel D, Weber W, Guilmette RA, Swanson J, Melo DR. Americium systemic biokinetic model for rats. Radiat Res 192:75–91; 2019.

Poudel D, Bertelli L, Klumpp JA, Dumit S, Waters TL. Biokinetics of 238Pu oxides: inferences from bioassay data. J. Radiol. Prot. 39:208-248; 2019.

Poudel D, Dumit S, Bertelli L, Miller G, Macsik Z, Klumpp JA. Dose Assessment Following a ^{238}Pu Inhalation Incident at Los Alamos National Laboratory. Health Phys [*ideally in the same issue as the present manuscript*]; 2022.

FIGURE CAPTIONS

Fig. 1. Rate of dissolution, approximate data and model.

Fig. 2. Dissolution fraction data used in this analysis.

Fig. 3. Posterior probability scatter plot for additional parameters distinguishing 4-component model from 3-component model. The points represent equally likely interpretations of the data and the box shows the extent of the prior.